Alzheimer's & Dementia®
THE JOURNAL OF THE ALZHEIMER'S ASSOCIATION

Aberrant crosstalk between insulin signaling and mTOR in young Down syndrome individuals revealed by neuronal-derived extracellular vesicles

Marzia Perluigi[1] | Anna Picca[2] | Elita Montanari[3] | Riccardo Calvani[2] | Federico Marini[4] | Roberto Matassa[5] | Antonella Tramutola[1] | Alberto Villani[6] | Giuseppe Familiari[5] | Fabio Di Domenico[1] | D. Allan Butterfield[7] | Kenneth J. Oh[8] | Emanuele Marzetti[2,9] | Diletta Valentini[6] | Eugenio Barone[1]

[1] Department of Biochemical Sciences "A. Rossi-Fanelli", Sapienza University of Rome, Rome, Italy

[2] Fondazione Policlinico Universitario Agostino Gemelli IRCCS, Rome, Italy

[3] Institute of Pharmaceutical Sciences, Department of Chemistry and Applied Biosciences, Zurich, Switzerland

[4] Department of Chemistry, Sapienza University of Rome, Roma, Italy

[5] Department of Anatomical, Histological, Forensic and Orthopedic SciencesSection of Human AnatomySapienza University of Rome, Rome, Italy

[6] Pediatric Unit, Bambino Gesù Children's Hospital-IRCCS, Rome, Italy

[7] Department of Chemistry and Sanders-Brown Center on Aging, University of Kentucky, Lexington, Kentucky, USA

[8] Bio-Rad Laboratories, Hercules, California, USA

[9] Università Cattolica del Sacro Cuore, Department of Geriatrics and Orthopedics, Rome, Italy

Correspondence
Eugenio Barone, Department of Biochemical Sciences "A. Rossi-Fanelli," Sapienza University of Rome, Piazzale Aldo Moro 5, 00185 Rome, Italy.
Email: eugenio.barone@uniroma1.it

Abstract

Introduction: Intellectual disability, accelerated aging, and early-onset Alzheimer-like neurodegeneration are key brain pathological features of Down syndrome (DS). Although growing research aims at the identification of molecular pathways underlying the aging trajectory of DS population, data on infants and adolescents with DS are missing.

Methods: Neuronal-derived extracellular vesicles (nEVs) were isolated form healthy donors (HDs, n = 17) and DS children (n = 18) from 2 to 17 years of age and nEV content was interrogated for markers of insulin/mTOR pathways.

Results: nEVs isolated from DS children were characterized by a significant increase in $pIRS1^{Ser636}$, a marker of insulin resistance, and the hyperactivation of the Akt/mTOR/p70S6K axis downstream from IRS1, likely driven by the higher inhibition of Phosphatase and tensin homolog (PTEN). High levels of $pGSK3\beta^{Ser9}$ were also found.

Conclusions: The alteration of the insulin-signaling/mTOR pathways represents an early event in DS brain and likely contributes to the cerebral dysfunction and intellectual disability observed in this unique population.

KEYWORDS
Alzheimer's disease, cognitive dysfunction, Down syndrome, Hsa21, insulin signaling, intellectual disability, mTOR, neurodegeneration, neurodevelopment, PTEN, trisomy 21

1 | BACKGROUND

Down syndrome (DS) is the most common genetic form of intellectual disability, caused by the triplication of chromosome 21 (Hsa21), with a prevalence of ≈12.8 per 10,000 births (≈1 in 780 newborns).[1]

The intellectual disability associated with DS likely results from alterations of brain development that can be traced back to fetal life stages. These alterations include widespread defects in neurogenesis, excessive numbers of astrocytes, dendritic atrophy, and impaired connectivity.[1,2]

HIGHLIGHTS

- Brain insulin resistance develops early in Down syndrome (DS) independent of peripheral alterations.
- Brain insulin resistance is associated with mTOR hyperactivation in DS.
- Neuronal-derived extracellular vesicles (nEVs) allow detection of alterations of the insulin/mTOR pathway in DS brain.
- PTEN inhibition drives insulin/mTOR alterations in DS brain.
- Alterations of the insulin/mTOR pathway allow discrimination of DS versus healthy individuals.

RESEARCH IN CONTEXT

1. Systematic review: The authors reviewed the literature using PubMed. The increased incidence of metabolic disorders in Down syndrome (DS) is documented, and several studies have examined metabolites and bioenergetic defects in the DS population. We have cited all the previous work. However, there is a substantial lack of evidence on the alteration of insulin and mTOR pathways in DS, particularly in the younger population.
2. Interpretation: This study shows that the analysis of nEVs can be used to detect early alterations of the insulin/mTOR pathway in the brain of young DS individuals. These alterations likely worsen intellectual disability in DS and may favor Alzheimer's disease (AD) development with age.
3. Future directions: The evaluation of nEVs content may be useful to identify novel targets for therapeutic interventions in DS. This aspect will be strengthened by performing additional studies to explore whether alterations identified through the analysis of nEVs associate with worse cognitive outcomes in DS.

Over the last decades, the lifespan of people with DS has significantly extended. However, the increased life expectancy brings about a higher risk of developing Alzheimer's disease (AD)–like dementia.[3,4] Due to the triplication of the amyloid precursor protein gene (*APP*) on Hsa21, DS may potentially be envisioned as a genetic form of AD, similar to its autosomal dominant form.[3, 4] Therefore, persons with DS represent a population to explore the molecular mechanisms underlying intellectual disability as well as neurodegeneration. Several studies have focused on the identification of neuronal pathways involved in synaptic plasticity, neurogenesis, and neurotransmission, which are altered early in life in people with DS.[3] However, no single gene or region of Hsa21 has been found to be responsible for all of the common features of DS.[5] This suggests that the coordination of multiple genes and other factors may be responsible for the development of major DS phenotypes.[3,6]

Previous studies support the idea that altered insulin signaling in the brain, referred to as brain insulin resistance, may affect the molecular pathways involved in synaptic plasticity and adult neurogenesis.[7] Indeed, the development of brain insulin resistance may lead to a reduction of "mindspan"—the ability of the brain to preserve mental capabilities throughout life—and increase the risk of neurodegeneration.[8] The mammalian target of rapamycin (mTOR) is a "master switch" between anabolic and catabolic cellular processes[9] through regulating glucose metabolism, bioenergetics, mitochondrial function, and autophagy, also in response to insulin.[10,11] mTOR has also been involved in long-lasting synaptic adaptations at the basis of higher-order brain function (ie, synaptic plasticity, memory preservation, and neuronal recovery).[10] Previous studies by our group and by others indicate that both insulin and mTOR signaling pathways are impaired early in life in the brain of people with DS[12,13] and DS animal models.[14–16] Moreover, crosstalk between insulin signaling and mTOR pathway has been indicated to play a key role in the maintenance of mindspan. Therefore, understanding at which time point and through which trajectory the disturbance of the insulin/mTOR pathway occurs and persists may indicate therapeutic targets against intellectual disability and neurodegeneration in people with DS.

In this regard, plasma-resident neuronal-derived extracellular vesicles (nEVs) show great potential as a diagnostic tool.[17] EVs are a heterogeneous population of vesicles released into the extracellular space by all cell types, including brain cells for cell-to-cell communication.[18] EVs carry surface markers and biologically active cargo molecules that are specific to their originating tissue/cell and that may reflect the tissue/cell's physiological state.[19,20] Thus the isolation of nEVs from the blood may provide a minimally invasive approach for sampling neuronal components in DS and may, therefore, be considered a form of "liquid biopsy."[20]

Recently, the characterization of nEVs cargo provided valuable information on the molecular alterations underlying AD neuropathology.[17,21] Increased levels of AD biomarkers, such as amyloid beta (Aβ) and phosphorylated tau (p-tau), were observed in nEVs from persons with AD relative to controls.[22,23] Furthermore, the analysis of nEVs collected from participants of the Baltimore Longitudinal Study of Aging revealed that markers of brain insulin resistance were among the strongest individual predictors of AD development, thereby highlighting a role for altered insulin signaling in AD onset and progression.[17] In addition, high levels of Aβ1-42, pTau181, and p-s396-Tau were identified in the nEVs of persons with DS compared with age-matched controls, already in childhood.[24]

Although a role for insulin/mTOR pathway during brain development and in the maintenance of brain functions has been proposed, no evidence is available in children with DS. In the present study, we applied a multiplex immunoassay for the simultaneous evaluation of all

the mediators of the insulin/mTOR pathway in circulating nEVs isolated from infants and adolescents with DS and age-matched controls.

2 | METHODS

2.1 | Study participants

For the present study, we enrolled infants and adolescents with DS (n = 18) and age-matched healthy donors (HDs, n = 17) from the Down Syndrome and Pediatric Outpatient Clinic of the Bambino Gesù Children's Hospital in Rome (Italy). The study was approved by the ethics committee of the Bambino Gesù Children Hospital (protocol ID # 1771_OPBG_2019). We have received and archived written consent for participation/publication from every individual whose data are included. Consent for inclusion in the study was obtained during a visit to outpatient clinics from all participants.

2.2 | nEV isolation

Blood samples were obtained from all participants after overnight fasting. All blood draws and processing followed established protocols using standard venipuncture procedures. Blood was collected in ethylenediaminetetraacetic acid (EDTA) polypropylene tubes, and was centrifuged at 850×g for 15 minutes at 4°C. Afterward, plasma was isolated and centrifuged again at 850×g for 15 minutes at 4°C to eliminate clots and aggregates. Plasma samples were then divided into 0.5-mL aliquots and stored at −80°C until analysis. Preanalytical factors for blood collection and storage complied with guidelines for EV biomarkers.[18] Evaluation of fasting glycemia and insulinemia (Table 1) was performed on the same plasma samples used to isolate nEVs. Homeostatic model assessment for insulin resistance (HOMA-IR) (Table 1) was then calculated by using the following formula: (fasting plasma insulin in mU/L × fasting plasma glucose in mmol/L)/22.5. nEV isolation was performed as described previously, with minor modifications.[17,25] Plasma samples were thawed on ice and defibrinated with thrombin (System Biosciences, Inc., Mountainview, CA) followed by 30 minutes of incubation at room temperature. Two-hundred fifty microliters of plasma were diluted 1:1 v/v with Dulbecco's calcium and magnesium-free salt solution (DSB, Thermo Scientific, Inc., Waltham, MA) with the addition of protease (#P8340, Sigma–Aldrich, St Louis, MO, USA) and phosphatase inhibitors (#P5726, Sigma–Aldrich, St Louis, MO, USA). Total EVs were collected using an Exo-spin Blood kit EX-02 (Cell Guidance, Cambridge, UK) according to the manufacturer's instructions, and finally resuspended in 0.5 mL of ultra-pure distilled water with the manufacturer-recommended concentration of protease and phosphatase inhibitors. To immunocapture L1 cell adhesion molecule (L1CAM)–positive nEVs, the suspension was incubated for 1 hour at 4°C with 4 μg of mouse anti-human CD171 (L1CAM) biotinylated antibody (clone 5G3) (Thermo Scientific, Inc.), followed by incubation with 25 μL of Pierce Streptavidin Plus UltraLink Resin (Thermo Scientific, Inc.) for 30 minutes at 4°C. After centrifuga-

TABLE 1 Demographic and anthropometric characteristics of controls (HD) and children with Down syndrome (DS)

	HD	DS	P
N	17	18	.81
Age range	4 – 17 years	2 – 16 years	
Age distribution (n)	0 – 5 years: 5	0 – 5 years: 8	
	6 – 11 years: 8	6 – 11 years: 4	
	12 – 17years: 4	12 – 17 years: 6	
Age (mean ± SD)	8.6 ± 4.4	8.7 ± 5.2	.68
Sex (M/F)	9/8	10/8	.88
Weight (mean, kg ± SD)	31.3 ± 16.2	30.2 ± 21.3	.33
Fasting glycemia (mean, mg/dL ± SD)	68.9 ± 12.7	64.6 ± 9.8	.16
Fasting insulin (mean, μU/mL ± SD)	8.9 ± 7.3	8.5 ± 4.5	.79
HOMA-IR	1.52 ± 1.08	1.50 ± 0.92	.95
BMI (kg/m^2, mean ± SD)	18.7 ± 5.2	19.8 ± 4.5	.18
Centile (mean ± SD)	59.8 ± 29.9	46.11 ± 25.5	.21
Obesity (n)	3	0	.06
Overweight (n)	3	1	.26
NAFLD (n)	0	0	n.s.

BMI, body mass index; HOMA-IR, homeostatic model assessment for insulin resistance; NAFLD, non-alcoholic fatty liver disease

tion at 800×g for 10 minutes at 4°C and removal of supernatant, nEVs were eluted with 200 μL of 0.1 M glycine. Beads were then sedimented by centrifugation at 4500×g for 5 minutes at 4°C, and the supernatants containing nEVs were transferred to clean tubes. pH was neutralized with 1 M Tris-HCl, and samples underwent two freeze/thaw cycles with M-PER protein extraction reagent (Thermo Scientific, Inc.) supplemented with protease and phosphatase inhibitors. The final suspensions containing nEVs proteins were stored at −80°C. Samples were thawed and vortexed twice prior to protein measurements. The stored suspensions were used to determine the total protein concentration by the Bradford assay (Pierce, Rockford, IL, USA). All investigators involved in nEV isolation and biomarker quantification were blinded until all measurements were completed.

2.3 | nEVs characterization by dynamic light scattering

Ten microliters of intact nEVs were used for the determination of the vesicle hydrodynamic diameter through dynamic light scattering (DLS). The mean hydrodynamic diameter (Z-average size), size distribution, and correlation curve of nEVs in phosphate-buffered saline (PBS; pH 7.2, dilution factor 1:100) were measured at 25°C using a Zetasizer Pro (Malvern Panalytical, UK) equipped with a solid state HeNe laser (λ = 632.8 nm) at the scattering angles of 173° and 13°. Size measurement data were analyzed by the general-purpose algorithm.

2.4 | nEV characterization by transmission electron microscopy

Intact nEVs were used for morphological evaluation of nEVs. The purified suspension stored at 4°C was deposited by drop casting on a Formvar copper grid and subsequently stained by Uranyless solution for 1 minute. Transmission electron microscopy (TEM) observations were performed using a Zeiss EM10 (Zeiss, Oberkochen, Germany) at 60 kV.

2.5 | nEVs characterization for EVs and neuronal markers

The detection of both transmembrane and intravesicular EV markers is required to confirm the sequential enrichment of EVs from neat plasma using Exo-spin Blood kit EX-02 sedimentation of total EVs followed by immunoprecipitation of nEVs. EV enrichment was confirmed by showing the presence of transmembrane (cluster of differentiation 81, CD81) and intravesicular EV markers (Alix) as well as the relative depletion of lipoprotein (apolipoprotein A1, APOA1) in both total and nEVs compared with EV-depleted plasma. Moreover, enrichment of EVs of neuronal origin was confirmed by evaluating L1CAM and neuronal nuclear protein (NeuN) levels, as neuronal markers, in nEVs, total EVs, and EV-depleted plasma samples. The evaluation of the markers mentioned above was performed by Western blot analysis described below.

2.6 | Western blot analysis

Ten micrograms of proteins for each sample were resolved on Criterion TGX Stain-Free 4-15% 18-well gel (Bio-Rad Laboratories, Hercules, CA, USA; #5678084) in a Criterion large format electrophoresis cell (Bio-Rad Laboratories, #1656001) in Tris/Glycine/SDS (TGS) Running Buffer (Bio-Rad Laboratories, #1610772). Immediately afterward, the gel was placed on a Chemi/UV/Stain-Free tray and visualized using a ChemiDoc MP imaging System (Bio-Rad Laboratories, #17001402) in a UV setting. Total protein load was assessed using the Image Lab Software (Bio-Rad Laboratories).

Subsequently, proteins were transferred via a TransBlot Turbo semi-dry blotting apparatus (Bio-Rad Laboratories, #1704150) onto nitrocellulose membranes (Bio-Rad laboratories, #162-0115). Membranes were blocked with 3% bovine serum albumin in 0.5% Tween-20/Tris-buffered saline (TBS-t) and incubated overnight at 4°C with the following antibodies: anti-CD81 (1:1000, Cell Signaling, Bioconcept, Allschwill, Switzerland, #56039S), anti-Alix (1:1000, Cell Signaling, Bioconcept, #2171S), anti-L1CAM (1:1000, Cell Signaling, #89861S), anti-APOA1 (1:2000, Thermo Scientific, Inc., #LF-MA0127), anti-NeuN (1:1000, Thermo Scientific, Inc., #702022), anti-Syntaxin-1A (1:1000, GeneTex, Irvine, CA, USA; #GTX113559), anti-PSD95 (1:1000, Cell Signalling, #3450S), and anti-phospho-CaMK IIα Thr286 (1:1000, Cell Signaling, #12716S). For L1CAM detection, an antibody targeting the C-terminal region of the protein was used, while nEVs were immunoprecipitated with an antibody targeting the N-terminal region (5G3).

After three washes with TBS-t buffer, membranes were incubated for 60 minutes at room temperature with the appropriate secondary antibodies conjugated with horseradish peroxidase (1:5000; Sigma–Aldrich, St. Louis, MO, USA). Membranes were developed with Clarity enhanced chemiluminescence (ECL) substrate (Bio-Rad Laboratories, #1705061), and the signal was acquired with Chemi-Doc MP (Bio-Rad Laboratories) and analyzed using Image Lab software (Bio-Rad Laboratories). Normalization was performed against total protein load signal.

2.7 | Bioplex assay

A magnetic bead–based immunoassay was used to measure levels of eight phosphoproteins and total target proteins pertaining to the mTOR signaling pathway in nEVs. All mediators were assayed in multiplex using the Bio-Plex Pro Cell Signaling protein kinase B (Akt) Panel, 8-plex (Bio-Rad Laboratories, #LQ00006JK0K0RR) to measure levels of the following phosphorylated proteins: insulin receptor substrate-1 at Ser363 (pIRS1^{Ser636}), phosphatase and tensin homolog at Ser380 (Phosphatase and tensin homolog (pPTEN)^{Ser380}), serine/threonine-protein kinase Akt-1 at Ser 473 (pAkt^{Ser473}), glycogen synthase kinase-3β at Ser9 (pGSK3β^{Ser9}), mTOR at Ser2448 (pmTOR^{Ser2448}), p70 S6 kinase at Thr389 (p70 S6 Kinase (pP70S6K)^{Thr389}), ribosomal protein S6 kinase beta-1 at Ser235/236 (pS6$^{Ser235/Ser236}$), and the Bcl2-associated agonist of cell death at Ser136 (pBAD^{Ser136}). Experiments were run on a Bio-Plex System with Luminex xMAP Technology (Bio-Rad Laboratories) and data were acquired on a Bio-Plex Manager Software 6.1 (Bio-Rad Laboratories) with instrument default settings. Median fluorescence intensities (MFI) corrected for the blank background were obtained for all analytes and results were calculated as the ratio between the MFI of phosphorylated targets and total proteins.

2.8 | Statistical analyses

Data were first tested for equal variance and normality (Shapiro-Wilk test). Data were not normally distributed and, therefore, the nonparametric Mann-Whitney test was used to compare participants with DS and healthy donors. A two-tailed alpha value of 0.05 was used to denote statistical significance.

Correlations were estimated by the Spearman test. Multivariate statistical modeling was then used to differentiate participants with DS and healthy donors based on levels of the measured mediators. A one-class classification strategy (also known as class-modeling), based on the use of the soft independent modeling of class analogies (SIMCA) method, was adopted.[26] SIMCA is particularly suitable for defining the salient traits of a target category, enabling one to verify whether new individuals are likely to belong to that same category or not. Mathematically, it operates by calculating a principal component (PC) model of the category of interest (in the present case, healthy donor group), and
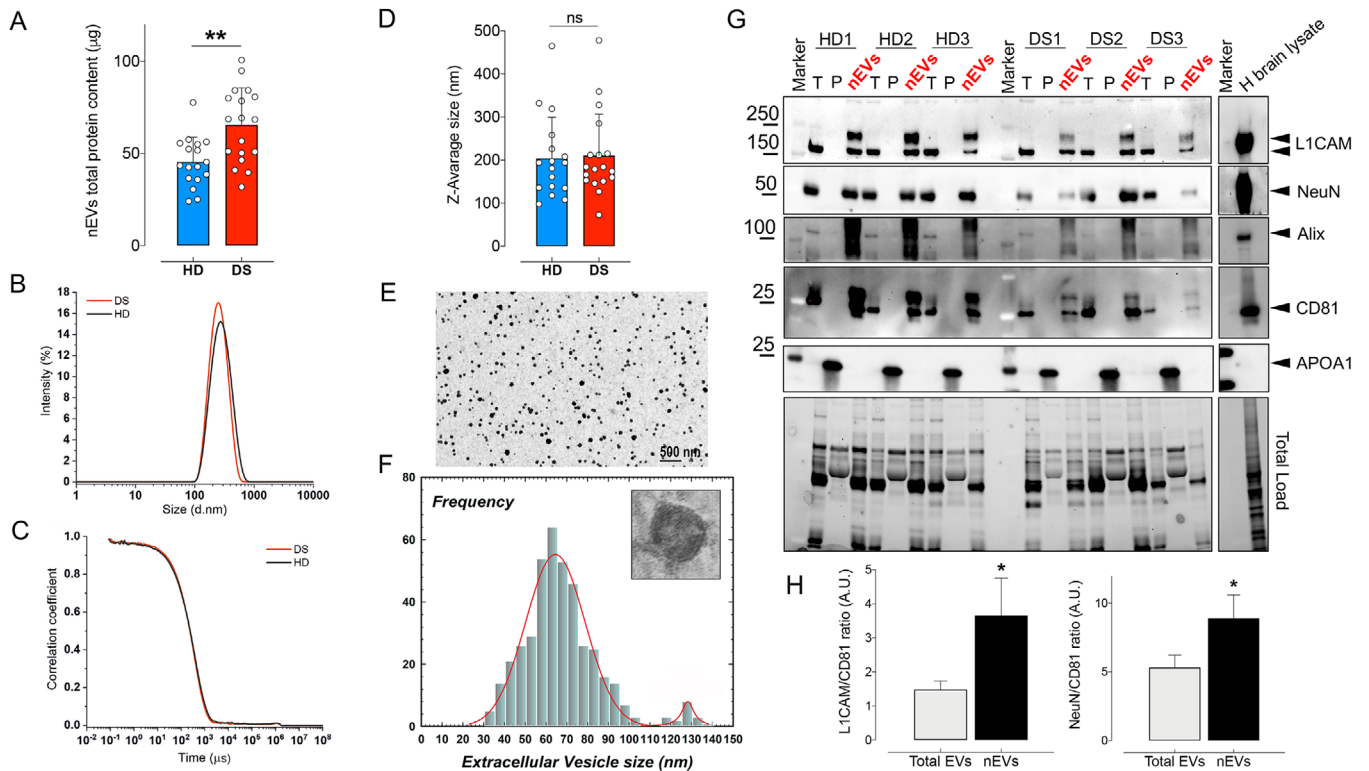
FIGURE 1 Characterization of the plasma-resident neuronal-derived extracellular vesicles (nEVs).. (A) Total protein content, (B) size distribution, (C) correlation curve, and (D) Z-average size (nm) of nEVs isolated from healthy donors (HDs) and participants with Down syndrome (DS). Error bars represent standard deviation (SD). In (E-F), morphological study of nEVs. BF-TEM image of nEVs (E). Plot showing the frequency distribution of the vesicle size histogram (F). Data fit by Gaussian convolution functions (red line). $P < .01$ statistically significant difference between experimental and theoretical data fitting. Furthermore, identification of nEV membranes evidences the presence of the bilayer membranes (inset in F). In (G), representative Western blot images of total EVs (T, isolated with Exo-spin Blood kit EX-02), EV-depleted plasma (P, supernatant after Exo-spin Blood kit EX-02), and nEVs (after immunocapture with L1CAM) isolated from HD (n = 3) and DS (n = 3) and probed for L1CAM, NeuN, Alix, CD81, and APOA1. The two bands detected for L1CAM in nEVs represent the non-glycosylated ($\sim\approx$170 kDa) and the glycosylated form ($\sim\approx$220 kDa). In (H), the degree of neuronal enrichment for nEVs compared to total EVs. L1CAM and NeuN and CD81 densitometric values were first normalized for total load and then both L1CAM and NeuN levels were expressed as a ratio with CD81. Data are presented as means $\pm$ SD. *$P < .05$ versus Total EVs (Mann-Whitney)

testing each new observation for its degree of deviation with respect to that model. Specifically, for each individual, a distance to the class model d is calculated as the combination of two test statistics, namely T^2, which accounts for the Mahalanobis distance of the sample's score to the center of the PC space, and Q, which corresponds to the squared residuals (ie, the squared Euclidean distance of the observation from its PC analysis projection). To make the two terms comparable, prior to being combined into the overall distance to the model, they are normalized by division to their critical value at 95% confidence. Accordingly, verification of whether an individual is likely to be part of the healthy donor class or not is based on assessing if the distance to the model is below a predefined criterion. In mathematical terms:

$$d_i = \sqrt{\left(T^2_{i,\,norm}\right)^2 + Q^2_{i,\,norm}} \leq \sqrt{2}$$

i indicating the generic i^{th} individual and the subscript *norm* explicitly referring to the above-mentioned normalization.

3 | RESULTS

3.1 | Demographics and clinical characteristics

Thirty-five participants ranging in age between 2 and 17 years, including 18 with DS and 17 controls, were enrolled and included in the analysis. Baseline characteristics of participants are listed in Table 1. Participants with and without DS did not differ for any demographic, clinical, or anthropometric characteristics.

3.2 | Characterization of nEVs

nEV preparations were characterized for protein content, size, and morphology through DLS and TEM, along with immunoblotting analyses for positive and negative EV markers, according to established criteria[18] (Figure 1).

Quantification of the nEVs was performed by measuring the total protein content, which provides an estimation of nEV amount.[18,27] Higher nEV levels were observed in participants with DS relative to controls ($P = .004$) (Figure 1A).

The size distribution of nEVs immunocaptured by L1CAM was studied with DLS (Figure 1A and 1B). Correlation coefficients of nEVs from both participant groups were consistent with EVs guidelines[18] and so were mean hydrodynamic diameter values (204 ± 95 nm and 210 ± 96 nm, in controls and participants with DS, respectively) (Figure 1C). The size of nEVs was comparable between the groups ($P = .77$).

Bright-field (BF) image TEM showed well-separated nEVs (Figure 1D). Imaging analyses were performed to accurately measure nEV size at low magnification to conduct the appropriate statistics.[28,29] Quantitative morphometric measurements were performed by generating a 2D contour map of 419 vesicles distributed on a probed area of 6220 nm per 4587 nm (Figure 1D). The analyzed size was plotted in a frequency profile of EVs with spherical shape. The bin distributions were processed by Gaussian fitting, and the frequency distribution of isolated nEVs was estimated to be centered around the mean value of 64 ± 0.71 nm, having a lowest polydispersity of about 1.10% (Figure 1E). Furthermore, small populations of bins were fitted to estimate a mean size of 128 ± 0.51 nm of the nEVs (Figure 1E). It should be noted that the mean hydrodynamic diameter of nEVs (detected by DLS measurements) was almost 3-fold greater than the size estimated with TEM, evidencing how the particle behaves in a fluid, thus taking into account the electric dipole layer that adheres to the vesicle surface.

The purification of nEVs was confirmed by Western blot analysis showing enrichment for transmembrane and intravesicular EV markers (ie, CD81 and Alix) and relative depletion of lipoprotein (ie, APOA1) in total EVs and nEVs compared with EV-depleted plasma (Figure 1F). A significant increase in neuronal markers levels, that is, L1CAM (nEVs/total EVs = 2.46) and NeuN (nEVs/total EVs = 1.67), in nEVs compared with total EVs and EV-depleted plasma confirmed the enrichment of nEVs by L1CAM immunoprecipitation (Figure 1G). The degree of neuronal enrichment is in line with previous studies reporting enrichment values from 1.6-fold to 5.6-fold depending on the marker.[20] In addition, the evaluation of the eluate from the L1CAM immunocapture of nEVs further reveals that nEVs are enriched in L1CAM and NeuN, whereas EV markers, that is, CD81 and Alix, can be observed in both nEVs and non-neuronal EVs (Supplementary Figure 1).

3.3 | nEV biomarker comparison between participants with DS and controls

The interrogation of nEVs for markers of the insulin/mTOR pathway revealed higher levels of pIRS1^{Ser636} (0.58 arbitrary units (A.U.) vs 0.23 A.U, $P = .041$), pPTEN^{Ser380} (0.48 A.U. vs 0.19 A.U, $P = .015$), pAkt^{Ser473} (0.15 A.U. vs 0.048 A.U, $P = .026$), pGSK3β^{Ser9} (0.036 A.U. vs 0.013 A.U, $P = .017$), pmTOR^{Ser2448} (0.055 A.U. vs 0.033 A.U, $P = .002$); pP70S6K^{Thr389} (0.21 A.U. vs 0.07 A.U, $P = .03$), pS6$^{Ser235/Ser236}$ (0.075 A.U. vs 0.019 A.U, $P = .02$), pBAD^{Ser136} (0.55 A.U. vs 0.24 A.U, $P = .03$) in participants with DS relative to controls (Figures 2B-I).

To evaluate whether alterations of the insulin/mTOR pathway were associated with synaptic defects in DS, levels of the three main synaptic proteins, that is, Syntaxin-1A (pre-synaptic), PSD95 (post-synaptic), and the active form of CamK IIα (pCamK IIα^{Thr286}, a central regulator of neuronal plasticity[30]), were evaluated. No significant differences were observed for Syntaxin-1A (1 A.U. vs 0.77 A.U., $P = .50$), PSD95 (1 A.U. vs 0.98 A.U., $P = .57$), or pCamK IIα^{Thr286} levels (1 A.U. vs 1.07 A.U., $P = .46$) between DS and controls (Supplementary Figure 2).

We also evaluated the levels of CD81 and L1CAM in nEVs and found no significant differences between participant groups (Supplementary Figure 3). To further confirm our results, we normalized insulin/mTOR pathway markers levels as well as those of synaptic proteins for both CD81 and L1CAM levels, as in previous reports.[18,31] Differences observed between DS and control participants remained significant after CD81 or L1CAM normalization (Supplementary Figures 3 - 5).

Taking advantage from the multiplexing property of the Luminex platform, we explored whether activation/inhibition of the above-mentioned mediators was consistent along the pathway. To this aim, correlation analyses were performed among nEV markers from both participant groups. Our findings show that nEV biomarkers are positively and significantly associated with one another in both participant groups, except for pmTOR^{Ser2448} versus pPTEN^{Ser380} ($P = .1$) and pmTOR^{Ser2448} versus pBAD^{Ser136} ($P = .1$) in participants with DS (Figures 3A-D). In addition, a strong negative association was found between pCamK IIα^{Thr286} and both pAkt^{Ser243} and pmTOR^{Ser2448} in controls but not in participants with DS (Figures 3A-D).

3.4 | nEV biomarker comparison between participants with DS and controls according to age

To verify whether the observed changes varied according to age, correlation analyses were performed. No significant associations with age were observed in either participant group (Figures 3A-D). Based on that, to unravel whether alterations in DS occur in childhood and remain consistent in older children and in adolescents independent of age, participants were categorized according to the age range reported in Table 1. Although differences were evident between DS and controls, the small sample size of each sub-group did not allow us to perform a reliable statistical analysis (data not shown). Hence, participant age was then categorized according to the median value (7 years for DS; 8 years for controls), and significantly higher levels of pIRS1^{Ser636} (0.57 A.U. vs 0.08 A.U., $P = .041$), pGSK3β^{Ser9} (0.024 A.U. vs 0.009 A.U., $P = .02$), pmTOR^{Ser2448} (0.69 A.U. vs 0.037 A.U., $P = .01$), and pS6$^{Ser235/Ser236}$ (0.06 A.U. vs 0.01 A.U., $P = .04$) were observed in participants with DS below the median age relative to their control peers (Figures 4A and 4C). A similar pattern was observed in participants above the median age, although differences did not reach statistical significance (Figure 4B). No significant differences were observed for any synaptic proteins (Supplementary Figure 6).
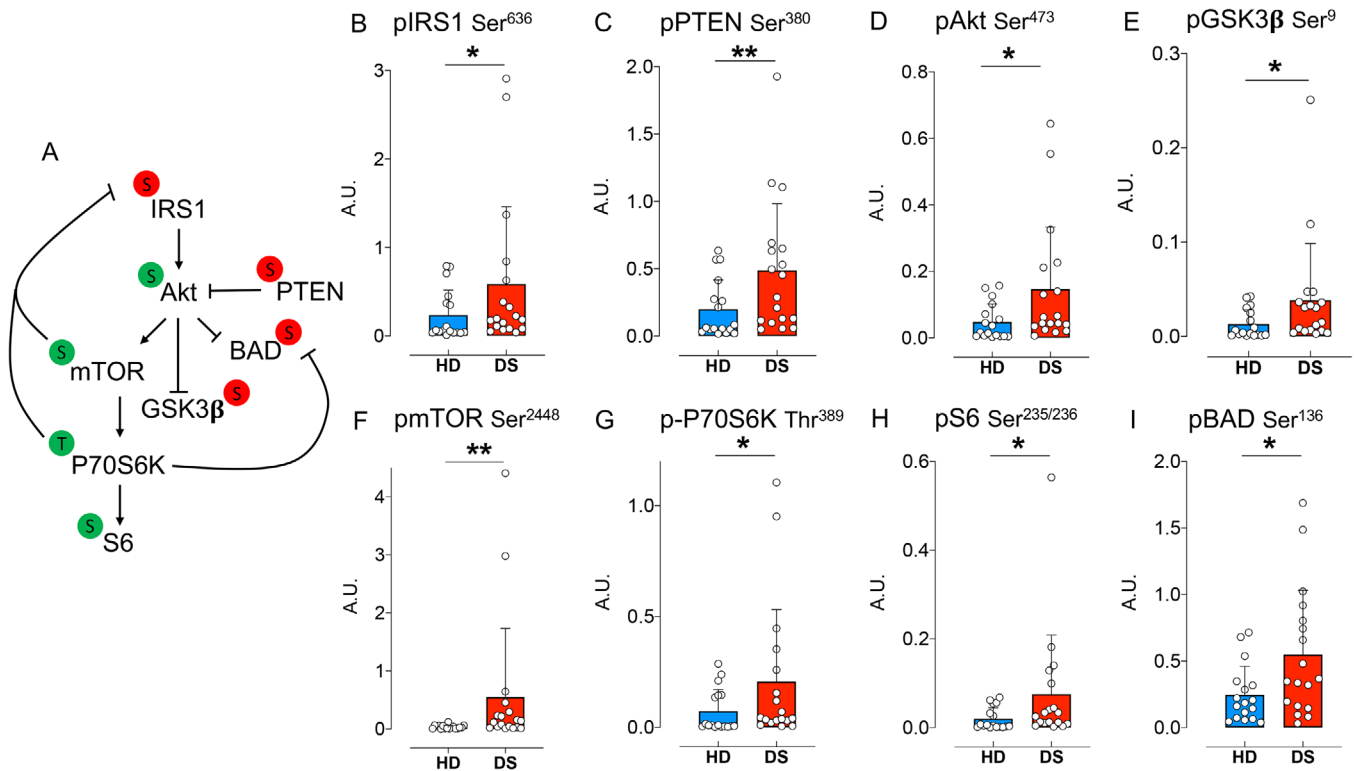
FIGURE 2 nEV biomarker levels in healthy donors (HDs) and children with Down syndrome (DS). (A) Schematic representation of the insulin/mTOR pathway. Arrows: activation; lines: inhibition; green circles: phosphorylation sites associated with protein activation; red circles: inhibitory phosphorylation sites. (B-I) Levels of biomarkers of the insulin/mTOR pathway evaluated in nEVs isolated from HD (n = 17) and DS (n = 18) children. Data are presented as means ± SD. *$P < .05$ and ** $P < .01$ versus HD (Mann-Whitney)

3.5 | SIMCA analysis

The whole set of measured mediator signals was used to build a multivariate classification model, with the aim of evaluating whether they could provide a differentiation between controls and participants with DS. Through the use of the SIMCA method, a model of the healthy donor class was built and cross-validated, and it was verified whether the model could recognize control individuals as part of the category (sensitivity) and DS participants as not (specificity). The optimal complexity of the PC model for the healthy donor class, after auto-scaling data pre-treatment, was found to be two components. Based on the model, it was possible to calculate the values of T^2_{norm} and Q_{norm} for each control and DS participant and, consequently, their distances to the category model. These results can be graphically visualized in Figure 5, where the cross-validated projections of controls and participants with DS onto the healthy donors model space are displayed. In the plot, the dashed black line corresponds to the decision threshold $d \leq \sqrt{2}$. In the calibration phase, the model was able to correctly recognize as healthy donors all control participants, corresponding to 100% sensitivity, while 2 of the 18 participants with DS were incorrectly accepted by the healthy donor class model, corresponding to a specificity of 88.9%. In cross-validation, 87.5% sensitivity and 85.4% specificity were obtained, as observable in Figure 5. The inspection of contributions of the individual variables to the value of T^2_{norm} and Q_{norm}[32] of participants with DS correctly identified as not belonging to the healthy

donor class suggests that in our DS population there are higher levels of pAkt[Ser473], pBAD[Ser136], pmTOR[Ser2448], pPTEN[Ser380].

Finally, a principal component analysis (PCA) was conducted to exclude that extreme values observed in DS population were outliers and thus can be kept in all the analyses (Supplementary Figure 7). PCA confirmed that extreme values are not outliers and likely account for the wide variability of pathological phenotypes of DS individuals that present with variable severity of clinical features[1,3].

4 | DISCUSSION

Our work reports for the first time a significant alteration of the insulin/mTOR pathway in infants and adolescents with DS through the analysis of nEVs. Furthermore, our data show that changes in the levels of protein phosphorylation are consistent across adjacent kinases of the insulin/mTOR pathway, indicating that the integrity of the signaling cascade is maintained in nEVs. Hence, nEVs are a valuable tool to investigate the neuronal insulin/mTOR pathway through a minimally invasive approach.

The first striking finding of our study is the significant IRS1 inhibition observed in nEVs from participants with DS. Inhibition of IRS1 is a marker of brain insulin resistance.[7] From a molecular point of view, IRS1[Ser636] phosphorylation is responsible for the uncoupling between insulin receptor (IR) and IRS1, which results in the inability of insulin
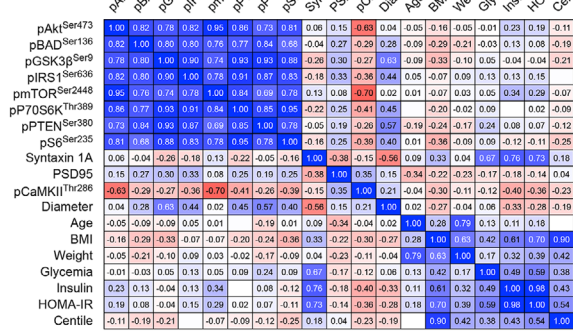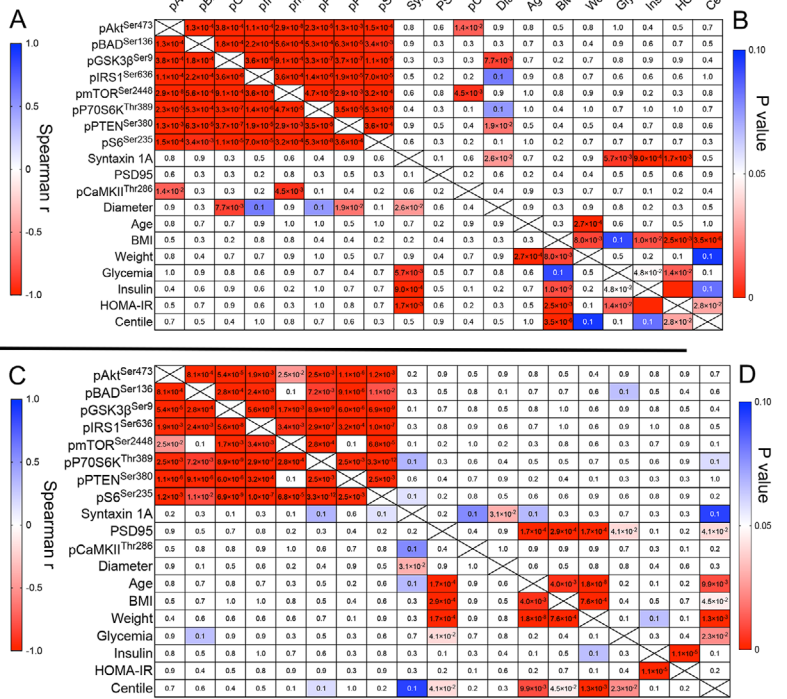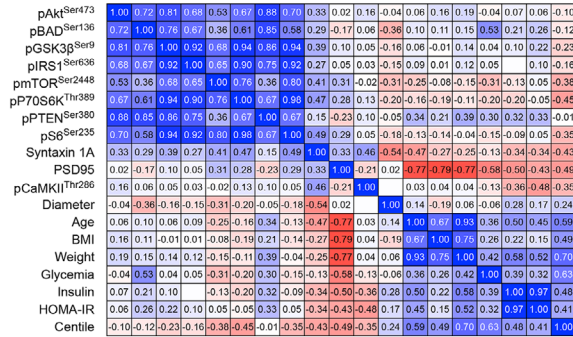
FIGURE 3 Correlation analyses in healthy donor (HD) and Down syndrome (DS) groups. Spearman correlation analyses were performed separately in HD (A-B) and DS groups (C-D) to explore associations among the biomarkers measured in nEVs as well as between biomarker levels and demographic characteristics of participants. Blue/white/red colors were used for the scheme. Blue represents the highest values, white the middle, and red the lower values both for Spearman *r* (A and C) and *P* values (B and D)

to activate the intracellular pathways downstream of IRS1.[11] Brain insulin resistance mediates synaptotoxic effects and leads to (1) synaptic loss, impaired autophagy, and increased neuronal apoptosis[7,8,33]; (2) increased production and secretion of Aβ peptides[7,34]; and (3) increased tau phosphorylation.[7,35,36] Of interest, all of the above-cited neuropathological alterations have been described in the brain of adult people with DS (reviewed in[3]). Moreover, these observations are in keeping with clinical studies showing that the failure in brain energy metabolism responsible for cognitive decline during aging or AD could be driven by the development of brain insulin resistance, particularly at early stages.[7,22]

In addition, IRS1 inhibition within the brain seems to occur independent of peripheral alterations. Fasting glycemia, insulinemia, and HOMA-IR—known to represent powerful risk factors for the development of brain insulin resistance and cognitive decline[7]—were within normal ranges and did not differ between participants with DS and controls. Similarly, metabolic disturbances/diseases associated with peripheral insulin resistance, such as overweight, obesity, type 2 diabetes, and non-alcoholic fatty liver disease, were not prevalent in our participant cohort.

Despite IRS1 inhibition, we observed that the activation of Akt, mTOR, and mTOR-associated targets, that is, P70S6K and S6, was consistently increased in nEVs isolated from participants with DS compared with controls, thus indicating an overactivated state. This observation confirms previous studies from ours and other groups show-

ing aberrant mTOR signaling in post-mortem brain from people with DS, with and without AD, and in AD brain.[12,37] Hyperactivation of mTOR has been associated with defects of autophagosome formation and autophagy and with accumulation of AD pathology markers.[1,2,14] Accordingly, published data show defects in endo-lysosomal pathways in DS[38–40] and efficacy of mTOR inhibitors to rescue this abnormality in primary fibroblast from persons with DS.[41] A protective role for EVs was previously proposed in DS by showing that higher EV release may be a mechanism to alleviate endo-lysosomal dysfunctions both in mice and humans.[27,42] Enhanced EVs secretion,[27,31,42] as observed also in our work, might serve as a delayed cellular response to reduce the size and number of endosomal compartments in DS by shedding more endosomal content into the brain extracellular space.[27,42] However, it is important to highlight that, in addition to the mean of increased nEVs release in DS, the analysis of nEV content provides information about the molecular alterations occurring within the brain, as we observed for the insulin/mTOR pathway, thus representing a powerful tool of investigation.

mTOR is involved in neuronal development and proper functioning of mature neurons,[43] and changes in mTOR activity are often observed in neurological diseases, including genetic disorders (eg, tuberous sclerosis and fragile X syndrome), epilepsy, brain tumors, and neurodegenerative disorders (AD, Parkinson disease, and Huntington disease).[44] The analysis of nEVs in children with DS, although at a different age, recapitulates the main findings obtained from post-mortem brain of
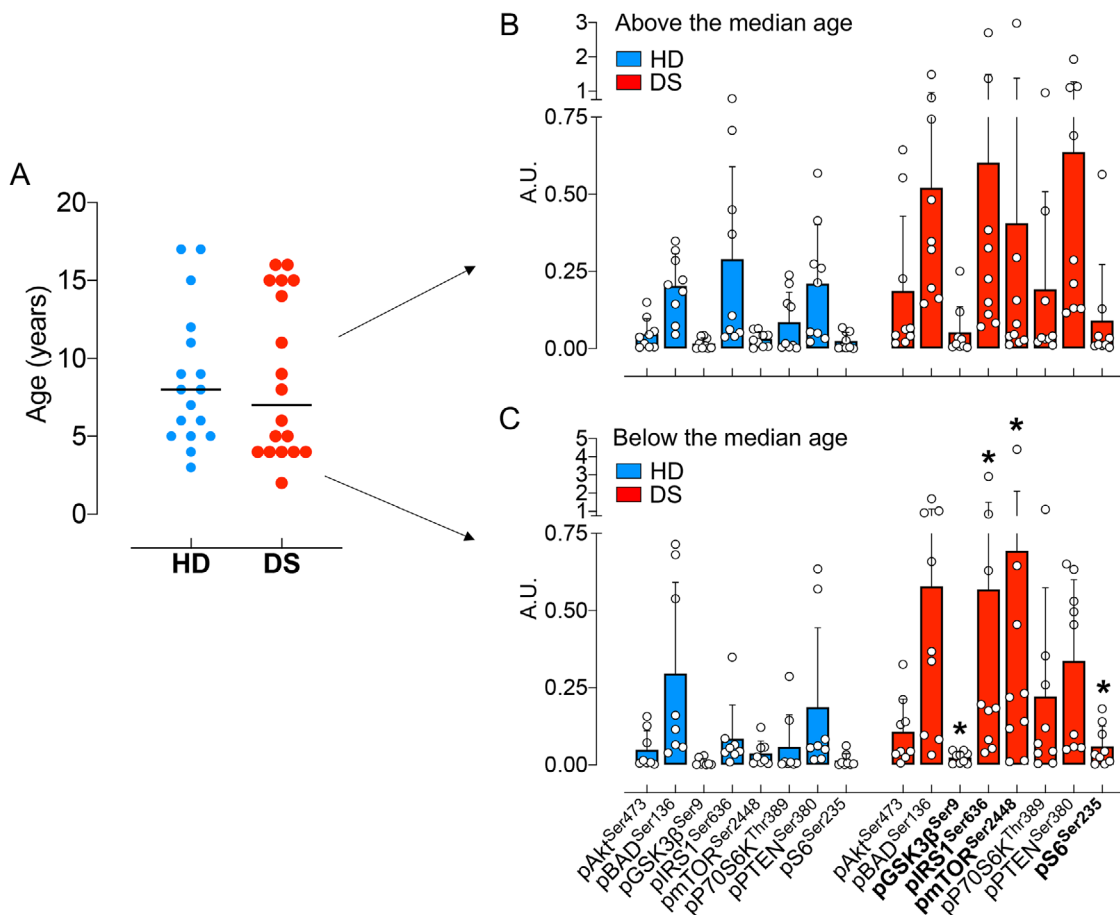
FIGURE 4 nEV biomarker levels in healthy donors (HDs) and children with Down syndrome (DS) by age category. (A) Levels of biomarkers for the insulin/mTOR pathway evaluated in nEVs isolated from HD and DS children were expressed by dividing the two groups into two further sub-groups according to the median age. Median age for HD was 8 years, while for DS children was 7 years. (B-C) Data of the two subgroups above the median age (HD = 9, DS = 9) are shown in (B), while those of the two subgroups below the median age (HD = 8, DS = 9) are shown in (C). Data are presented as means ± SD. *P < .05 versus HD (Mann-Whitney)

people with DS.[12,45] This is in line with our previous findings and further confirms the reliability of shuttling EVs as a source of disease biomarkers.

Not surprisingly, the hyperactivation of mTOR/P70S6K axis may be responsible for the observed IRS1 inhibition in DS, similar to what was reported for AD.[37,46,47] Although this feedback loop is intrinsic to the physiology of insulin signaling, considering that mTOR/P70S6K dampens excessive IRS1 activation,[11] a chronic hyper-activation is detrimental.[11] Within this picture, a role for increased Aβ levels may also be suggested, since Aβ oligomers were demonstrated to both promote IRS1 inhibition[48] and mTOR hyperactivation[49] in AD. Thus aberrant, chronic mTOR hyperactivation diverts the feedback mechanism into reduced insulin sensitivity and leads to a harmful synergistic path affecting neuronal functions in DS.[10]

In addition to that, the hyperactivation of Akt/mTOR axis may contribute to dysfunctional synaptic plasticity mechanisms in DS through CaMK IIα. CaMK IIα is a central regulator of neuronal plasticity and cognitive functions, such as learning.[30] Both insulin and nutrients promote a transient increase of intracellular Ca^{2+} levels (that activates CamK IIα) along with the activation of the Akt/mTOR axis.[30,50] Conversely, mTOR activation leads to CaMK IIα inhibition through a feedback mechanism, thus contributing to CamK IIα regulation.[30] Both hyperactivation and sustained inhibition of CaMK IIα are detrimental to neurons and synaptic plasticity.[51] Hence, the lack of correlations that we found in DS suggest that crosstalk between the insulin/mTOR pathway and CaMK IIα may be disrupted in DS, which might contribute to intellectual disability.

Hyperactivation of the Akt/mTOR axis might also be responsible for increased BAD phosphorylation observed in nEVs isolated from participants with DS. Indeed, both Akt and P70S6K are known to phosphorylate BAD to promote anti-apoptotic signals and, thus, cell survival.[52,53] This is the first observation of increased BAD inhibition in DS and is in agreement with the concept that compensatory events promote survival mechanisms prior to the development of AD pathology both in persons with DS and transgenic mice.[54–56] Moreover, we previously reported that pro-apoptotic signals were significantly increased in persons with DS only after the development of AD pathology.[57]

In the search for putative candidates responsible for the impairment of insulin/mTOR pathway crosstalk, we suggest that PTEN may play a role. PTEN is a widely known negative regulator of insulin/PI3K
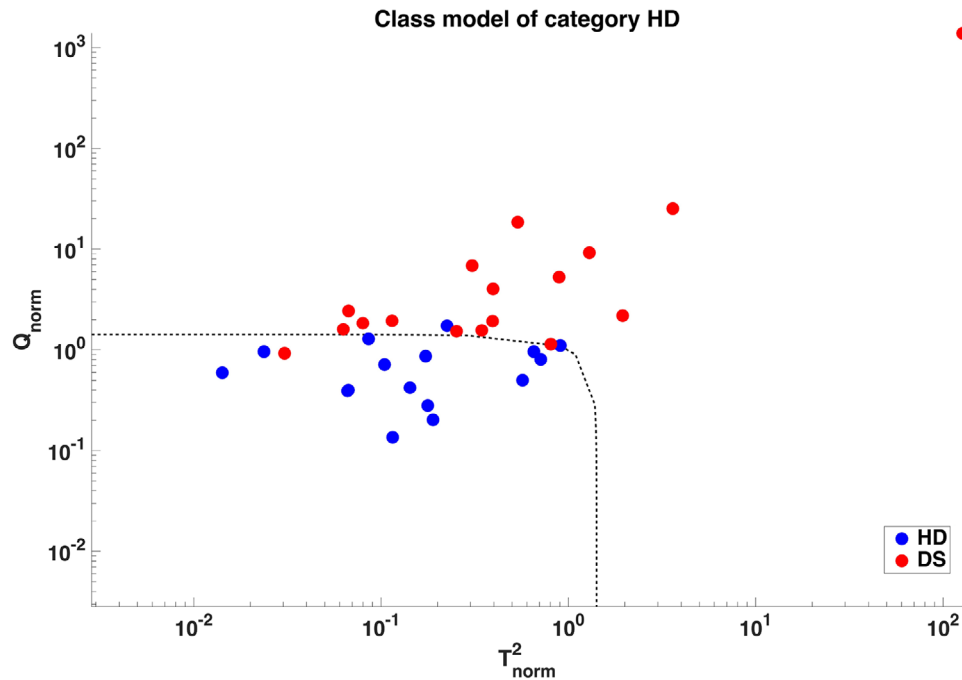
FIGURE 5 SIMCA model: cross-validated projection of the samples onto the space of the healthy donor (HD) category. In the space spanned by the two variables T^2_{norm} and Q_{norm}, the region associated with the class HD is represented by the area below the dashed black line identifying the classification threshold. The plot shows that almost all HD participants (blue circles), falling below the line, are correctly identified as members of the class. Likewise, the majority of participants with DS (red circles), falling above the decision line, are correctly identified as not being HD

signaling.[58,59] We hypothesize that the significant PTEN inhibition (pPTEN[Ser380]) observed in nEVs from participants with DS would lead to an accumulation of phosphatidylinositol-3, 4, 5-triphosphate (PIP3), responsible for sustained overactivation of Akt and its downstream targets, that is, mTOR. A dysregulation of the axis is also supported by the lack of a significant association between PTEN and either mTOR[Ser2448] or BAD[Ser136] in participants with DS, but not in controls, as well as by SIMCA results, suggesting that PTEN inhibition may promote an unchecked Akt hyperactivation, which further contributes to aberrant mTOR activation and BAD inhibition. This proposed scenario is reinforced by recent observations showing that PTEN inhibition is coupled with Akt/mTOR hyperactivation in post-mortem brain samples obtained from people with DS and AD.[12,37,45]

Observations from the current study also suggest that alterations of the insulin/mTOR pathway occur quite early in DS brain, already during the childhood. Because people with DS show intellectual disability ranging from mild to severe with cognitive functions below chronological age expectations[60] and because the insulin/mTOR pathway regulates processes associated with neuronal plasticity,[7,8] we propose that our results may add new insight about the molecular mechanisms responsible for worse cognitive performance in DS children. We acknowledge that one limitation of the current study is the lack of correlations with cognitive measures, such as mental age or memory and learning, and further research is warranted to fully understand the pathophysiologic processes behind our observations.

In conclusion, our findings contribute to expand the knowledge on the neuropathological alterations in DS brain by analyzing a very young

population still poorly characterized. As discussed earlier, defects of insulin/mTOR pathway, besides being involved in cognitive dysfunctions, are associated with the onset of AD. The pathophysiology of AD in DS is similar to that of the sporadic and autosomal dominant forms of AD (reviewed in[61]). Although longitudinal studies of AD in people with DS exist,[62] the natural history of biomarker changes in DS has not been established except that in the adult population.[4] Hence, we propose that the analysis of nEVs may lead to the identification of novel disease biomarkers early in life that may also become targets for therapeutic development in DS.

CONFLICTS OF INTEREST

The authors disclose that this work was supported by Jerome-Lejeune Foundation grant no. 1887-BE2019B to EB and MP; Fondi Ateneo grant funded by Sapienza University no. RM11715C77336E99 to EB and no. C26H15JT9X to MP; NIH grants no. R56AG055596 and AG060056 to DAB.

Furthermore,

• Eugenio Barone was recipient of the following grants during the past 36 months:

REFERENCES

1. Antonarakis SE, Skotko BG, Rafii MS, et al. Down syndrome. *Nat Rev Dis Primers.* 2020; 6: 9.
2. Stagni F, Giacomini A, Emili M, Guidi S, Bartesaghi R. Neurogenesis impairment: an early developmental defect in Down syndrome. *Free Radic Biol Med.* 2018; 114: 15-32.
3. Lott IT, Head E. Dementia in Down syndrome: unique insights for Alzheimer disease research. *Nat Rev Neurol.* 2019; 15: 135-147.
4. Fortea J, Vilaplana E, Carmona-Iragui M, et al. Clinical and biomarker changes of Alzheimer's disease in adults with Down syndrome: a cross-sectional study. *Lancet.* 2020; 395: 1988-1997.
5. Korbel JO, Tirosh-Wagner T, Urban AE, et al. The genetic architecture of Down syndrome phenotypes revealed by high-resolution analysis of human segmental trisomies. *Proc Natl Acad Sci U S A.* 2009; 106: 12031-12036.
6. Dierssen M, Fructuoso M, Martinez de Lagran M, Perluigi M, Barone E. Down Syndrome Is a Metabolic Disease: altered Insulin Signaling Mediates Peripheral and Brain Dysfunctions. *Front Neurosci.* 2020; 14: 670.
7. Arnold SE, Arvanitakis Z, Macauley-Rambach SL, et al. Brain insulin resistance in type 2 diabetes and Alzheimer disease: concepts and conundrums. *Nat Rev Neurol.* 2018; 14: 168-181.
8. Spinelli M, Fusco S, Grassi C. Brain insulin resistance and hippocampal plasticity: mechanisms and biomarkers of cognitive decline. *Front Neurosci.* 2019; 13: 788.
9. Condon KJ, Sabatini DM. Nutrient regulation of mTORC1 at a glance. *J Cell Sci.* 2019: 132.
10. Switon K, Kotulska K, Janusz-Kaminska A, Zmorzynska J, Jaworski J. Molecular neurobiology of mTOR. *Neuroscience.* 2017; 341: 112-153.
11. White MF, Copps KD. The mechanisms of insulin action. *Endocrinol Adult Pediatr (Seventh Edition).* 2016: 556-585.e13. 2016.
12. Perluigi M, Pupo G, Tramutola A, et al. Neuropathological role of PI3K/Akt/mTOR axis in Down syndrome brain. *Biochim Biophys Acta.* 2014; 1842: 1144-1153.
13. Iyer AM, van Scheppingen J, Milenkovic I, et al. mTOR hyperactivation in down syndrome hippocampus appears early during development. *J Neuropathol Exp Neurol.* 2014; 73: 671-683.
14. Tramutola A, Lanzillotta C, Barone E, et al. Intranasal rapamycin ameliorates Alzheimer-like cognitive decline in a mouse model of Down syndrome. *Transl Neurodegener.* 2018; 7: 28.
15. Di Domenico F, Tramutola A, Barone E, et al. Restoration of aberrant mTOR signaling by intranasal rapamycin reduces oxidative damage: focus on HNE-modified proteins in a mouse model of down syndrome. *Redox Biol.* 2019; 23: 101162.
16. Lanzillotta C, Tramutola A, Di Giacomo G, et al. Insulin resistance, oxidative stress and mitochondrial defects in Ts65dn mice brain: a harmful synergistic path in down syndrome. *Free Radic Biol Med.* 2021; 165: 152-170.
17. Kapogiannis D, Mustapic M, Shardell MD, et al. Association of extracellular vesicle biomarkers with Alzheimer disease in the Baltimore Longitudinal Study of Aging. *JAMA Neurol.* 2019.
18. Thery C, Witwer KW, Aikawa E, et al. Minimal information for studies of extracellular vesicles 2018 (MISEV2018): a position statement of the International Society for Extracellular Vesicles and update of the MISEV2014 guidelines. *J Extracell Vesicles.* 2018; 7: 1535750.

19. Kowal J, Arras G, Colombo M, et al. Proteomic comparison defines novel markers to characterize heterogeneous populations of extracellular vesicle subtypes. *Proc Natl Acad Sci U S A*. 2016; 113: E968-77.

20. Mustapic M, Eitan E, Werner JK Jr, et al. Plasma extracellular vesicles enriched for neuronal origin: a potential window into brain pathologic processes. *Front Neurosci*. 2017; 11: 278.

21. Mullins RJ, Mustapic M, Goetzl EJ, Kapogiannis D. Exosomal biomarkers of brain insulin resistance associated with regional atrophy in Alzheimer's disease. *Hum Brain Mapp*. 2017; 38: 1933-1940.

22. Eren E, Hunt JFV, Shardell M, et al. Extracellular vesicle biomarkers of Alzheimer's disease associated with sub-clinical cognitive decline in late middle age. *Alzheimers Dement*. 2020; 16: 1293-1304.

23. Kapogiannis D, Boxer A, Schwartz JB, et al. Dysfunctionally phosphorylated type 1 insulin receptor substrate in neural-derived blood exosomes of preclinical Alzheimer's disease. *FASEB J*. 2015; 29: 589-596.

24. Hamlett ED, Goetzl EJ, Ledreux A, et al. Neuronal exosomes reveal Alzheimer's disease biomarkers in Down syndrome. *Alzheimers Dement*. 2017; 13: 541-549.

25. Mansur RB, Delgado-Peraza F, Subramaniapillai M, et al. Exploring brain insulin resistance in adults with bipolar depression using extracellular vesicles of neuronal origin. *J Psychiatr Res*. 2021; 133: 82-92.

26. De Luca S, Bucci R, Magrì AD, Marini F, Class Modeling Techniques in Chemometrics: Theory and Applications. 2018.

27. Gauthier SA, Perez-Gonzalez R, Sharma A, et al. Enhanced exosome secretion in Down syndrome brain - a protective mechanism to alleviate neuronal endosomal abnormalities. *Acta Neuropathol Commun*. 2017; 5: 65.

28. Matassa R, Orlanducci S, Reina G, et al. Structural and morphological peculiarities of hybrid Au/nanodiamond engineered nanostructures. *Sci Rep*. 2016; 6: 31163.

29. Reina G, Tamburri E, Orlanducci S, et al. Nanocarbon surfaces for biomedicine. *Biomatter*. 2014; 4: e28537.

30. Takahara T, Amemiya Y, Sugiyama R, Maki M, Shibata H. Amino acid-dependent control of mTORC1 signaling: a variety of regulatory modes. *J Biomed Sci*. 2020; 27: 87.

31. Hamlett ED, Ledreux A, Potter H, et al. Exosomal biomarkers in Down syndrome and Alzheimer's disease. Free Radic. *Biol Med*. 2018; 114: 110-121.

32. Westerhuis JA, Gurden SP, Smilde AK. Generalized contribution plots in multivariate statistical process monitoring. *Chemometr Intell Lab Syst*. 2000; 51: 95-114.

33. Butterfield DA, Di Domenico F, Barone E. Elevated risk of type 2 diabetes for development of Alzheimer disease: a key role for oxidative stress in brain. *Biochim Biophys Acta*. 2014; 1842: 1693-1706.

34. Triani F, Tramutola A, Di Domenico F, et al. Biliverdin reductase-A impairment links brain insulin resistance with increased Abeta production in an animal model of aging: implications for Alzheimer disease. *Biochim Biophys Acta Mol Basis Dis*. 2018; 1864: 3181-3194.

35. Sharma N, Tramutola A, Lanzillotta C, et al. Loss of biliverdin reductase-A favors Tau hyper-phosphorylation in Alzheimer's disease. *Neurobiol Dis*. 2019; 125: 176-189.

36. Imamura T, Yanagihara YT, Ohyagi Y, et al. Insulin deficiency promotes formation of toxic amyloid-beta42 conformer co-aggregating with hyper-phosphorylated tau oligomer in an Alzheimer's disease model. *Neurobiol Dis*. 2020; 137: 104739.

37. Tramutola A, Triplett JC, Di Domenico F, et al. Alteration of mTOR signaling occurs early in the progression of Alzheimer disease (AD): analysis of brain from subjects with pre-clinical AD, amnestic mild cognitive impairment and late-stage AD. *J Neurochem*. 2015; 133: 739-749.

38. Cataldo AM, Mathews PM, Boiteau AB, et al. Down syndrome fibroblast model of Alzheimer-related endosome pathology: accelerated endocytosis promotes late endocytic defects. *Am J Pathol*. 2008; 173: 370-384.

39. Jiang Y, Sato Y, Im E, et al. Lysosomal dysfunction in Down syndrome is APP-dependent and mediated by APP-betaCTF (C99). *J Neurosci*. 2019; 39: 5255-5268.

40. Botte A, Laine J, Xicota L, et al. Ultrastructural and dynamic studies of the endosomal compartment in Down syndrome. *Acta Neuropathol Commun*. 2020; 8: 89.

41. Bordi M, Darji S, Sato Y, et al. mTOR hyperactivation in Down syndrome underlies deficits in autophagy induction, autophagosome formation, and mitophagy. *Cell Death Dis*. 2019; 10: 563.

42. Perez-Gonzalez R, Gauthier SA, Sharma A, et al. A pleiotropic role for exosomes loaded with the amyloid beta precursor protein carboxyl-terminal fragments in the brain of Down syndrome patients. *Neurobiol Aging*. 2019; 84: 26-32.

43. Perluigi M, Di Domenico F, Butterfield DA. mTOR signaling in aging and neurodegeneration: at the crossroad between metabolism dysfunction and impairment of autophagy. *Neurobiol Dis*. 2015; 84: 39-49.

44. Ryskalin L, Limanaqi F, Frati A, Busceti CL. Fornai F. mTOR-related brain dysfunctions in neuropsychiatric disorders. *Int J Mol Sci*. 2018: 19.

45. Tramutola A, Lanzillotta C, Di Domenico F, et al. Brain insulin resistance triggers early onset Alzheimer disease in Down syndrome. *Neurobiol Dis*. 2020; 137: 104772.

46. Barone E, Di Domenico F, Cassano T, et al. Impairment of biliverdin reductase-A promotes brain insulin resistance in Alzheimer disease: a new paradigm. *Free Radic Biol Med*. 2016; 91: 127-142.

47. Caccamo A, Belfiore R, Oddo S. Genetically reducing mTOR signaling rescues central insulin dysregulation in a mouse model of Alzheimer's disease. *Neurobiol Aging*. 2018; 68: 1.

48. Bomfim TR, Forny-Germano L, Sathler LB, et al. An anti-diabetes agent protects the mouse brain from defective insulin signaling caused by Alzheimer's disease- associated Abeta oligomers. *J Clin Invest*. 2012; 122: 1339-1353.

49. Norambuena A, Wallrabe H, McMahon L, et al. mTOR and neuronal cell cycle reentry: how impaired brain insulin signaling promotes Alzheimer's disease. *Alzheimers Dement*. 2017; 13: 152-167.

50. Williams AJ, Umemori H. The best-laid plans go oft awry: synaptogenic growth factor signaling in neuropsychiatric disease. *Front Synaptic Neurosci*. 2014; 6: 4.

51. Bayer KU, Kinase SchulmanHCaM. Still Inspiring at 40. *Neuron*. 2019; 103: 380-394.

52. Harada H, Andersen JS, Mann M, Terada N, Korsmeyer SJ. p70S6 kinase signals cell survival as well as growth, inactivating the pro-apoptotic molecule BAD. *Proc Natl Acad Sci U S A*. 2001; 98: 9666-9670.

53. Datta SR, Dudek H, Tao X, et al. Akt phosphorylation of BAD couples survival signals to the cell-intrinsic death machinery. *Cell*. 1997; 91: 231-241.

54. Aziz NM, Guedj F, Pennings JLA, Olmos-Serrano JL, Siegel A, Haydar TF, et al. Lifespan analysis of brain development, gene expression and behavioral phenotypes in the Ts1Cje, Ts65Dn and Dp(16)1/Yey mouse models of Down syndrome. *Dis Model Mech*. 2018: 11.

55. Head E, Lott IT, Patterson D, Doran E, Haier RJ. Possible compensatory events in adult Down syndrome brain prior to the development of Alzheimer disease neuropathology: targets for nonpharmacological intervention. *J Alzheimers Dis*. 2007; 11: 61-76.

56. Tramutola A, Falcucci S, Brocco U, et al. Protein oxidative damage in UV-related skin cancer and dysplastic lesions contributes to neoplastic promotion and progression. *Cancers (Basel)*. 2020; 12(1): 110.

57. Tramutola A, Pupo G, Di Domenico F, et al. Activation of p53 in Down syndrome and in the Ts65Dn mouse brain is associated with a proapoptotic phenotype. *J Alzheimers Dis*. 2016; 52: 359-371.

58. Knafo S, Esteban JA. PTEN: local and global modulation of neuronal function in health and disease. *Trends Neurosci*. 2017; 40: 83-91.

59. Chen Z, Dempsey DR, Thomas SN, Hayward D, Bolduc DM, Cole PA. Molecular features of phosphatase and Tensin Homolog (PTEN) regulation by C-terminal phosphorylation. *J Biol Chem.* 2016; 291: 14160-14169.

60. Edgin JO. Cognition in Down syndrome: a developmental cognitive neuroscience perspective. *Wiley Interdiscip Rev Cogn Sci.* 2013; 4: 307-317.

61. Snyder HM, Bain LJ, Brickman AM, et al. Further understanding the connection between Alzheimer's disease and Down syndrome. *Alzheimers Dement.* 2020; 16: 1065-1077.

62. Devenny DA, Silverman WP, Hill AL, Jenkins E, Sersen EA, Wisniewski KE. Normal ageing in adults with Down's syndrome: a longitudinal study. *J Intellect Disabil Res.* 1996; 40(Pt 3): 208-221.

SUPPORTING INFORMATION

Additional supporting information may be found in the online version of the article at the publisher's website.